ACS Macro Letters

Letter

pubs.acs.org/macroletters

Cross Nucleation in Polyethylene with Precisely Spaced Ethyl Branches

Yoshinobu Nozue,*[,†] Shuichiro Seno,[†] Tatsuhiro Nagamatsu,[†] Satoru Hosoda,[†] Yuya Shinohara,[‡] Yoshiyuki Amemiya,[‡] E. B. Berda,[§,∥] G. Rojas,[§,⊥] and K. B. Wagener*[,§]

[†]Petrochemicals Research Laboratory, Sumitomo Chemical Co., Ltd., Kitasode, Chiba, Japan

[‡]Department of Advanced Materials Science, Graduate School of Frontier Sciences, The University of Tokyo, Kashiwa, Chiba, Japan

[§]Department of Chemistry, University of Florida, Gainesville, Florida 32611-7200, United States

ABSTRACT: In cross nucleation, an early nucleating crystalline polymorph (A) nucleates another crystalline polymorph (B) of higher or lower thermodynamic stability without undergoing a polymorphic transformation. Although this phenomenon was recently observed in the crystallization process of several small molecules, there has been insufficient evidence for cross nucleation in a crystalline polymer. In this paper, we report cross nucleation behavior during an isothermal crystallization of a crystalline polymer with precisely spaced branches. Polyethylene with ethyl branches on every 21st carbon exhibited growth of new spherulites at the growth front of an initially formed spherulite. The radial growth rate of the initially formed spherulite and the newly grown spherulite calculated from polarized optical microscope data were 0.76 μm/min and 1.01 μm/min, respectively. The growth rate of the newly grown spherulite is faster than that of the initially formed spherulite, which meets a required condition for cross nucleation. Scanning microbeam wide-angle X-ray scattering (WAXS) confirmed that the crystalline polymorphs of the two kinds of spherulites are not the same.

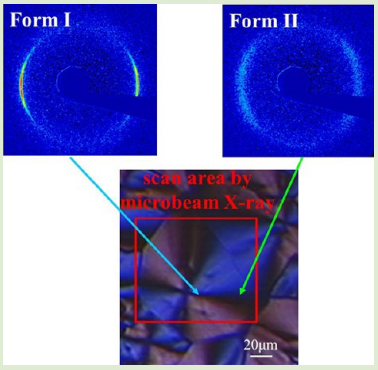

In cross nucleation, an early nucleating crystalline polymorph (A) nucleates another crystalline polymorph (B) of higher or lower thermodynamic stability without undergoing a polymorphic transformation.[1] This phenomenon has been recently reported in several small molecules, such as D-mannitol and D-sorbitol.[1−5] For cross nucleation to occur, the growth rate of polymorph (B) should be faster than that of polymorph (A).[1,2,4,5] Chen et al.[2] studied the crystallization of 5-methyl-2-[(2-nitrophenyl)amino]-3-thiophenecarbonitrile (ROY) with and without annealing and observed that the efficiency of cross nucleation is related to the crystalline perfection of polymorph (A). They also confirmed that the degree of lattice matching between polymorphs (A) and (B) is not an important factor in cross nucleation.[2]

A report by Fraschini et al.[6] suggests that cross nucleation occurs in the crystalline polymer, poly(1,3-dioxolan) (PDOL). Under polarized optical microscope (POM) observation, phase III of PDOL grew from the growth front of phase IIb under isothermal crystallization conditions. However, phases IIb and III appeared to be the same crystalline polymorph, but with different thermal stabilities, due to the difference in the lamella thickness of the two phases. Farrance et al.[7] reported two-stage crystal growth in polyhydroxybutyrate. The process is similar to cross nucleation when a free surface is present. However, two-stage growth in the polyhydroxybutyrate system seems to originate from the difference between the flat-on and edge-on lamellae of the same polymorph. In linear polyethylene under high pressure, Rastogi and Kurelec[8] reported that the hexagonal phase grows on the substrate of the orthorhombic phase that is not formed via nucleation and growth but by transformation from the hexagonal phase. However, to our knowledge, there has been no report of a crystalline polymer having an early nucleating crystalline polymorph which nucleates another crystalline polymorph without undergoing a polymorphic transformation.

This paper provides the first confirmation of cross nucleation in a crystalline polymer. We have found that cross nucleation occurs in polyethylene (PE) with short chain alkyl branches placed at precise intervals along the chain. The branched PE samples were synthesized by ADMET polymerization technology[9−12] with either ethyl branches precisely spaced on every 21st carbon (EB21) or with hexyl branches on every 21st carbon (HB21). The weight-averaged molecular weight (M_w) and the distribution (M_w/M_n) were M_w = 33 000 and M_w/M_n = 2.0 in EB21 and M_w = 40 000 and M_w/M_n = 1.55 in HB21. The observed transition peak temperatures during cooling (T_c) and heating (T_m) and the corresponding enthalpies measured by DSC were T_c = 11 °C, ΔH_c = 64.3 J/g, T_m = 24 °C, and ΔH_m = 65.0 J/g in EB21 and T_c = 1 °C, ΔH_c = 51.6 J/g, T_m = 12 °C, and ΔH_m = 52.0 J/g in HB21. As was previously reported,[13] the transition detected by DSC is not the crystallization/melting but mesophase (hexagonal phase) formation/melting. EB21 and HB21 show crystallization mediated by a transient hexagonal phase under isothermal crystallization conditions

Received: May 1, 2012
Accepted: May 30, 2012
Published: June 8, 2012

   dx.doi.org/10.1021/mz300215u | *ACS Macro Lett.* 2012, 1, 772−775

near the T_c detected by DSC. It was reported that the ethyl branch in EB21 can be incorporated into the crystal, resulting in the formation of thicker lamellae, while the hexyl branch in HB21 is sterically hindered from being incorporated into the crystal.[13,14]

EB21 crystallized into the hexagonal phase under isothermal conditions in the range of 5−17 °C, while by X-ray scattering at 21−28 °C crystallization through nucleation and growth was observed, but not crystallization mediated by a hexagonal mesophase. Figure 1 shows the results of small-angle X-ray

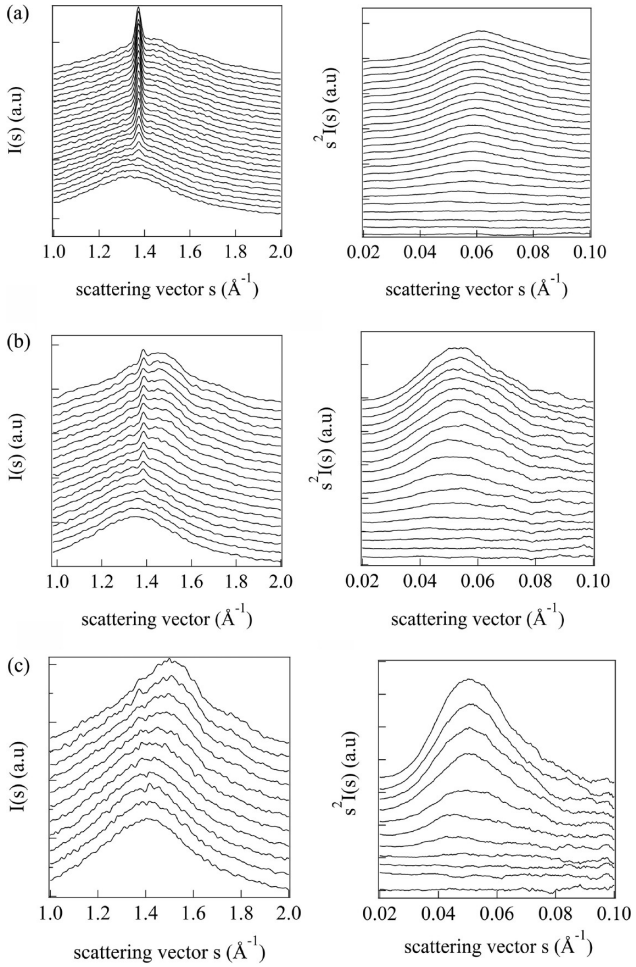

Figure 1. WAXS (left) and SAXS (right) changes of EB21 isothermally crystallized at (a) 21 °C, (b) 25 °C, and (c) 28 °C.

scattering (SAXS) and wide-angle X-ray scattering (WAXS) simultaneous measurements during the isothermal crystallization of EB21 at 21, 25, and 28 °C. The observed WAXS intensity profiles depend on the isothermal crystallization temperature. The crystalline form with one sharp peak at 1.37 Å^{-1} (defined as form I), and a long period of 115 Å was observed at 21 °C, while at 28 °C there were two broad peaks at around 1.48 and 1.71 Å^{-1} (defined as form II) with a long period of 125 Å, clearly indicating that EB21 has at least two crystalline forms. Interestingly, forms I and II coexist at 25 °C. Using the WAXS data obtained at 25 °C, we separated each crystalline peak through curve fitting using three Lorentz functions for crystalline peaks and one Gauss function for an amorphous peak. Figure 2 shows a plot of integrated scattering intensity versus time for each crystalline form during isothermal

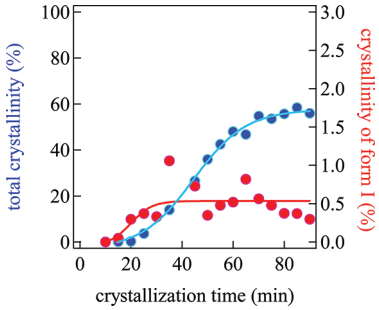

Figure 2. Total crystallinity (blue circles) and crystallinity of form I (red circles) during isothermal crystallization at 25 °C.

crystallization. Form I initially nucleates and grows to a small extent, followed by the growth of the form II, which is the major polymorph at this temperature.

The spherulite growth behavior of EB21 at 25 °C was observed under POM. Figure 3 shows new spherulites growing from the growth front of the initially formed spherulite (white arrows); this behavior is quite similar to the cross nucleation observed in D-mannitol.[1] The interface between the initial and the newly grown spherulites is zigzag-shaped, as shown by the dashed arrows in Figure 3f. The radial growth rates of the initial and newly grown spherulites calculated from the POM data

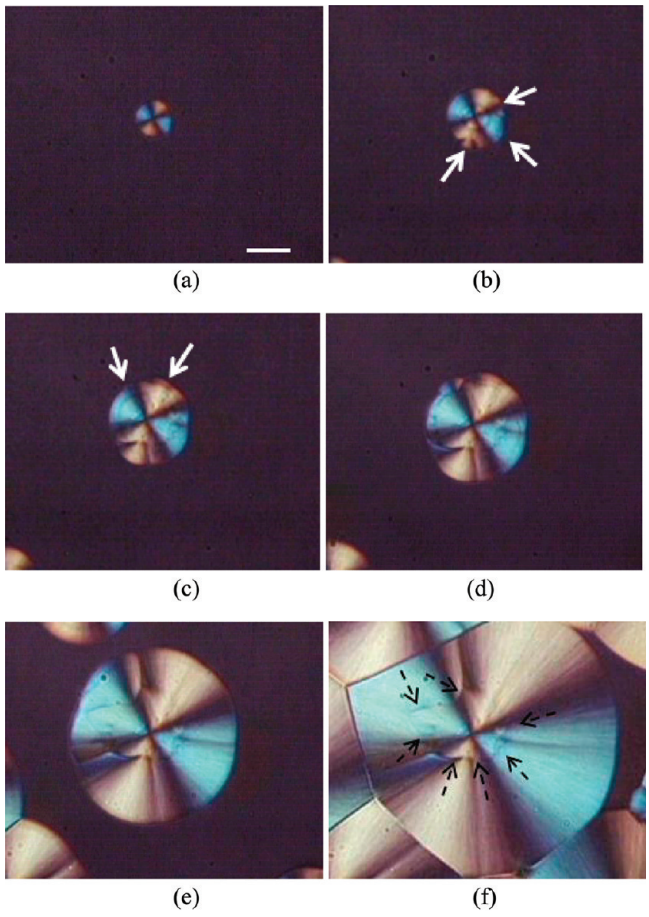

Figure 3. Spherulite growth via cross nucleation during isothermal crystallization at 25 °C [(a) 13 min, (b) 19 min, (c) 25 min, (d) 30 min, (e) 45 min, and (f) 73 min] observed by POM. Arrows show the newly grown spherulites from the growth front of an initially formed spherulite. Dashed arrows show the zigzag-shaped boundary.

dx.doi.org/10.1021/mz300215u | ACS Macro Lett. 2012, 1, 772−775

were 0.76 μm/min and 1.01 μm/min, respectively, clearly meeting the required condition of more rapid growth for the second spherulite.

To identify the crystalline form of each spherulite, the sample isothermally crystallized at 25 °C was scanned by microbeam X-rays (5 μm × 5 μm beam size), and the WAXS data were recorded at local regions of the spherulites. Figure 4 shows a

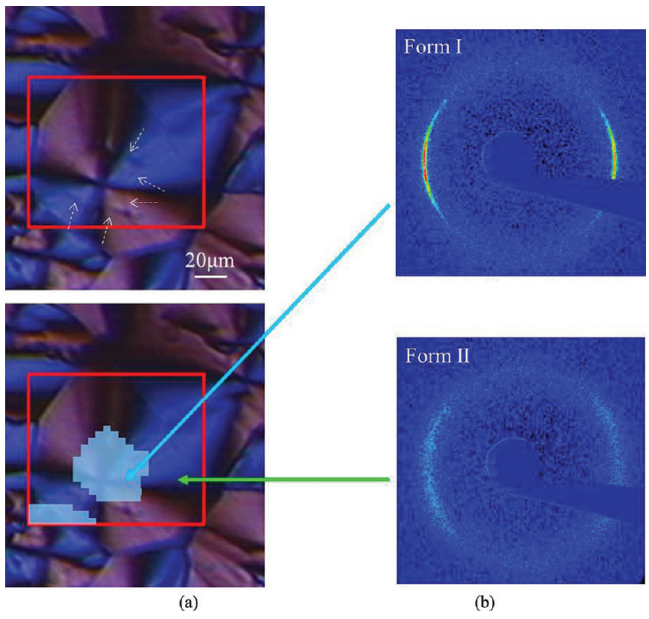

Figure 4. POM image of EB21 isothermally crystallized at 25 °C and used for microbeam X-ray scattering measurements (upper part of a). The red square region was scanned with microbeam X-ray. Dotted arrows in the upper part of a point to a zigzag shaped boundary between forms I and II. The light blue colored region inside red square in lower part of a is the region where diffraction of form I was mainly observed. Typical diffraction of form I (upper b) and form II (lower b).

POM picture of the spherulites used in the microbeam X-ray scattering experiment; the region inside of the red square was scanned by microbeam X-rays at 5 μm intervals. WAXS corresponding to the form I was observed at the central region marked with light blue, while WAXS corresponding to the form II was obtained in the surrounding region. A closer look of the upper part of Figure 4a reveals a zigzag-shaped line, which has a good correspondence with the spatial distribution of forms I and II (see the lower part of Figure 4a). Thus, the zigzag-shaped lines observed in Figures 3 and 4 correspond to the boundary between form I and form II spherulites. This correspondence is quite similar to the POM image of D-mannitol containing 10% (w/w) poly(vinylpyrrolidone) (see Figure 1c of ref 4). These results clearly indicate that the new form II spherulite is formed through cross nucleation from the growth front of the form I spherulite, initially observed under isothermal crystallization conditions at 25 °C.

The mechanism for cross nucleation of EB21 is proposed as follows. At 25 °C, the lamella thickness roughly evaluated from long period (121 Å) and the crystallinity (55%) is 66 Å. Assuming a trans zigzag structure, the interval between ethyl branches in the EB21 main chain is about 30 Å. Thus, the observed lamella thickness indicates that two ethyl branches are involved in one stem of a lamella crystal. Form I has a highly ordered packing structure along the axis corresponding to the diffraction peak at 1.37 $Å^{-1}$, and it is plausible to assign this peak to the 010 diffraction of the triclinic phase, based on a previous report.[15] On the other hand, the WAXS of form II shows no sharp diffraction peak, and the packing structure is not well-ordered along any crystalline axis.

Based on these data, we consider the reason why form II grows faster than form I. According to the Lauritzen–Hoffman theory,[16] after the attachment of a polymer stem to the flat growth front as a secondary nucleus, additional stems spread out laterally through folding.

Microbeam X-ray scattering indicates that form I has a very ordered packing structure along the *b*-axis, which is the radial growth direction of a form I spherulite. In form I, the ethyl branches are likely oriented along the *a*-axis, instead of the *b*-axis, because ethyl branches incorporated into the crystal strongly perturb the crystalline packing structure. The direction along the *a*-axis is parallel to a lateral growth direction of the secondary nucleated stem, and the ethyl branch is considered to disturb the attachment of the stem onto the site next to the secondary nucleus of form I. This means that the ethyl branches selectively oriented along the *a*-axis disturb the lateral growth of the secondary nucleus, resulting in the slower radial growth rate of form I. On the other hand, in form II, the packing structure is disordered along all (a, b, and c) axes. Thus, the ethyl branches in form II are considered not to have a strongly preferred direction, and the lateral growth of a second nucleus of form II will be faster than the growth of form I. It should also be noted that the hexagonal mesophase with disordered packing structure grows faster than the ordered orthorhombic phase in linear PE.[8] In the formation of the disordered packing phase, low selectivity in chain orientation is sufficient during packing formation. Thus, the disordered packing phase may need less time to grow.

With respect to the primary nucleation, it is known that a cylindrical nucleus has a critical free energy of

$$F = \frac{8\pi\sigma_f\sigma_l{}^2(T_m^0)^2}{(\Delta H)^2(\Delta T)^2} \quad (1)$$

where ΔH is the latent heat of fusion; $\Delta T = T^0{}_m - T_c$ is the degree of supercooling; and σ_f and σ_l are surface tensions at the fold and lateral surfaces, respectively.[17] In form I, nuclei may be produced with larger ΔH or smaller σ_f and σ_l compared to form II. A precise crystal structure determination is needed for more complete understanding.

In the computer simulation study of cross nucleation using the sphere model, it was reported that the free energy difference between polymorphs associated with cross nucleation is small.[18] To obtain information about the thermal stabilities of the two forms, isothermal crystallization at 25 °C was continued for 6 h, and then the sample was melted at a rate of 5 °C/min. It was observed by POM that forms I and II melted almost simultaneously at around 36–37 °C (data not shown), indicating that their thermal stabilities are about the same, in accord with the simulation study. We can consider two possibilities about the comparable thermal stabilities of the two crystalline forms. One possibility is that the crystal free energy of form I itself is almost equal to that of form II at the same thickness. Since the sharp peak for form I corresponds to 010 diffraction, the polymorph is highly ordered along the *b*-axis. On the other hand, the packing order along the other two axes may be very low due to the inclusion of two ethyl branches per stem, making the total free energy of form I high in spite of the

dx.doi.org/10.1021/mz300215u | ACS Macro Lett. 2012, 1, 772–775

highly ordered *b*-axis. Therefore, the free energy of form I is comparable to that of form II with low packing order along any axis. The other possibility is that the form with higher latent heat of fusion has thinner lamella than the other.

The results presented in this paper confirm that cross nucleation can occur in a crystalline polymer. However, the dominant factors involved in cross nucleation are still unclear, and the reason that this phenomenon is observed for EB21 is still not well understood. More detailed analyses of crystal structure, such as packing structure and lamella thickness, are needed to further elucidate the nature of this phenomenon.

EXPERIMENTAL METHODS

SAXS-WAXS simultaneous measurements were performed at BL-15A in the Photon Factory of KEK (Tsukuba). The beam was collimated with the bending mirror and monochromator. The X-ray wavelength was 1.50 Å, and the beam size at the sample position was about 500 μm × 500 μm. SAXS and WAXS camera lengths were calibrated with Silver Behenate diffraction rings. Two PILATUS 100K-S (DECTRIS Ltd., Switzerland) were used for the SAXS and WAXS data acquisition, respectively. A temperature-controlling stage (Linkam Scientific Instruments Ltd., THMS-600), which can control the sample temperature within rates of 0.01−130 °C/min, was used as the sample cell. Samples for X-ray measurement were sandwiched between thin mica plates. EB21 was initially held at 50 °C for 10 min, and then the temperature was dropped to the isothermal crystallization temperature at a rate of 100 °C/min.

The microbeam WAXS measurement was performed at BL-4A[19] in the Photon Factory. At BL-4A, the X-ray beam was focused to 5 × 5 μm^2 at the sample position with a Kirkpatrick−Baez mirror. The details of the experimental setup at BL-4A are described in our previous report.[20] The thin sample for microbeam WAXS was prepared by stretching the molten EB21 at 100 °C by spatula on a piece of glass sheet with 30 μm thickness (Matsunami Glass Ind., Ltd.). The temperature-controlling stage specified above was used to control the sample temperature. EB21 was initially held at 50 °C for 10 min, and then the temperature was dropped to 25 °C at a rate of 100 °C/min. After the impingement of a growing spherulite, the scanning experiment was performed. With the X-ray microbeam, the region of interest was scanned with a step of 5 μm. X-ray diffraction data were recorded by a charge-coupled device (CCD) detector coupled with an X-ray image intensifier.[21]

POM measurements were performed using an OLYMPUS microscope and a CCD camera. The temperature-controlling stage was used to control the sample temperature, and the thermal history was same as that in the microbeam X-ray scattering measurement.

AUTHOR INFORMATION

Corresponding Author

*Y.N., address: Sumitomo Chemical Co., Ltd., Petrochemicals Research Laboratory, 2-1 Kitasode, Sodegaura City, Chiba 299-0295, Japan. E-mail: nozue@sc.sumitomo-chem.co.jp. K.B.W., address: University of Florida, Department of Chemistry, Gainesville, FL 32611-7200. E-mail: wagener@chem.ufl.edu.

Present Addresses

[‖]Department of Chemistry and Materials Science Program, University of New Hampshire, Durham, New Hampshire 03824, United States.

[⊥]The Colombian Sugar Cane Research Center, Calle 58N #3BN-110, Cali, Colombia.

Notes

The authors declare no competing financial interest.

ACKNOWLEDGMENTS

The experiments at the Photon Factory were performed under the approval of the Photon Factory Program Advisory Committee (Proposal No.: 2010G540). This material is based upon work supported by the National Science Foundation under Grant No. DMR-0703261. Any opinions, findings, and conclusions or recommendations expressed in this material are those of the author(s) and do not necessarily reflect the views of the National Science Foundation. This material is based upon catalyst work supported by, or in part by, the U.S. Army Research Laboratory and the U.S. Army Research Office under Grant No. W911NF-09-1-0290.

REFERENCES

(1) Yu, L. *J. Am. Chem. Soc.* **2003**, *125*, 6380.
(2) Chen, S.; Xi, H.; Yu, L. *J. Am. Chem. Soc.* **2005**, *127*, 17439.
(3) Stoica, C.; Tinnermans, P.; Meekes, H.; Vlieg, E.; van Hoof, P. J. C. M.; Kaspersen, F. M. *Cryst. Growth Des.* **2005**, *5*, 975.
(4) Tao, J.; Yu, L. *J. Phys. Chem.* **2006**, *110*, 7098.
(5) Yu, L. *CrystEngComm* **2007**, *9*, 847.
(6) Fraschini, C.; Jiménez, L.; Kalala, B.; Prud'homme, R. E. *Polymer* **2012**, *53*, 188.
(7) Farrance, O. E.; Jones, R. A. L.; Hobbs, J. K. *Polymer* **2009**, *50*, 3730.
(8) Rastogi, S.; Kurelec, L. *J. Mater. Sci.* **2000**, *35*, 5121.
(9) Smith, J. A.; Brzezinska, K. R.; Valenti, D. J.; Wagener, K. B. *Macromolecules* **2000**, *33*, 3781.
(10) Sworen, J. C.; Wagener, K. B. *Macromolecules* **2007**, *40*, 4414.
(11) Rojas, G.; Wagener, K. B. *Macromolecules* **2009**, *42*, 1934.
(12) Rojas, G.; Berda, E. B.; Wagener, K. B. *Polymer* **2008**, *49*, 2985.
(13) Nozue, Y.; Kawashima, Y.; Seno, S.; Nagamatsu, T.; Hosoda, S.; Berda, E. B.; Rojas, G.; Baughman, T. W.; Wagener, K. B. *Macromolecules* **2011**, *44*, 4030.
(14) Hosoda, S.; Nozue, Y.; Kawashima, Y.; Utsumi, S.; Nagamatsu, T.; Wagener, K. B.; Berda, E. B.; Rojas, G.; Baughman, T. W. *Macromol. Symp.* **2009**, *282*, 50.
(15) Lieser, G.; Wegner, G.; Smith, J. A.; Wagener, K. B. *Colloid Poym. Sci.* **2004**, *282*, 773.
(16) Lauritzen, J. I.; Hoffman, J. D. *J. Res. Natl. Bur. Stand.* **1960**, *64A*, 73.
(17) Muthukumar, M. Nucleation in Polymer Crystallization. In *Advances in Chemical Physics*, Vol. *128*; Rice, S. A., Ed.; John Wiley & Sons, Inc.: Hoboken, NJ, 2004.
(18) Desgranges, C.; Delhommelle, J. *J. Am. Chem. Soc.* **2006**, *128*, 10368.
(19) Iida, A.; Noma, T. *Nucl. Instrum. Methods* **1993**, *B82*, 129.
(20) Nozue, Y.; Kurita, R.; Hirano, S.; Kawasaki, N.; Ueno, S.; Iida, A.; Nishi, T.; Amemiya, Y. *Polymer* **2003**, *44*, 6397.
(21) Amemiya, Y.; Ito, K.; Yagi, N.; Asano, Y.; Wakabayashi, K.; Ueki, T.; Endo, T. *Rev. Sci. Instrum.* **1995**, *66*, 2290.